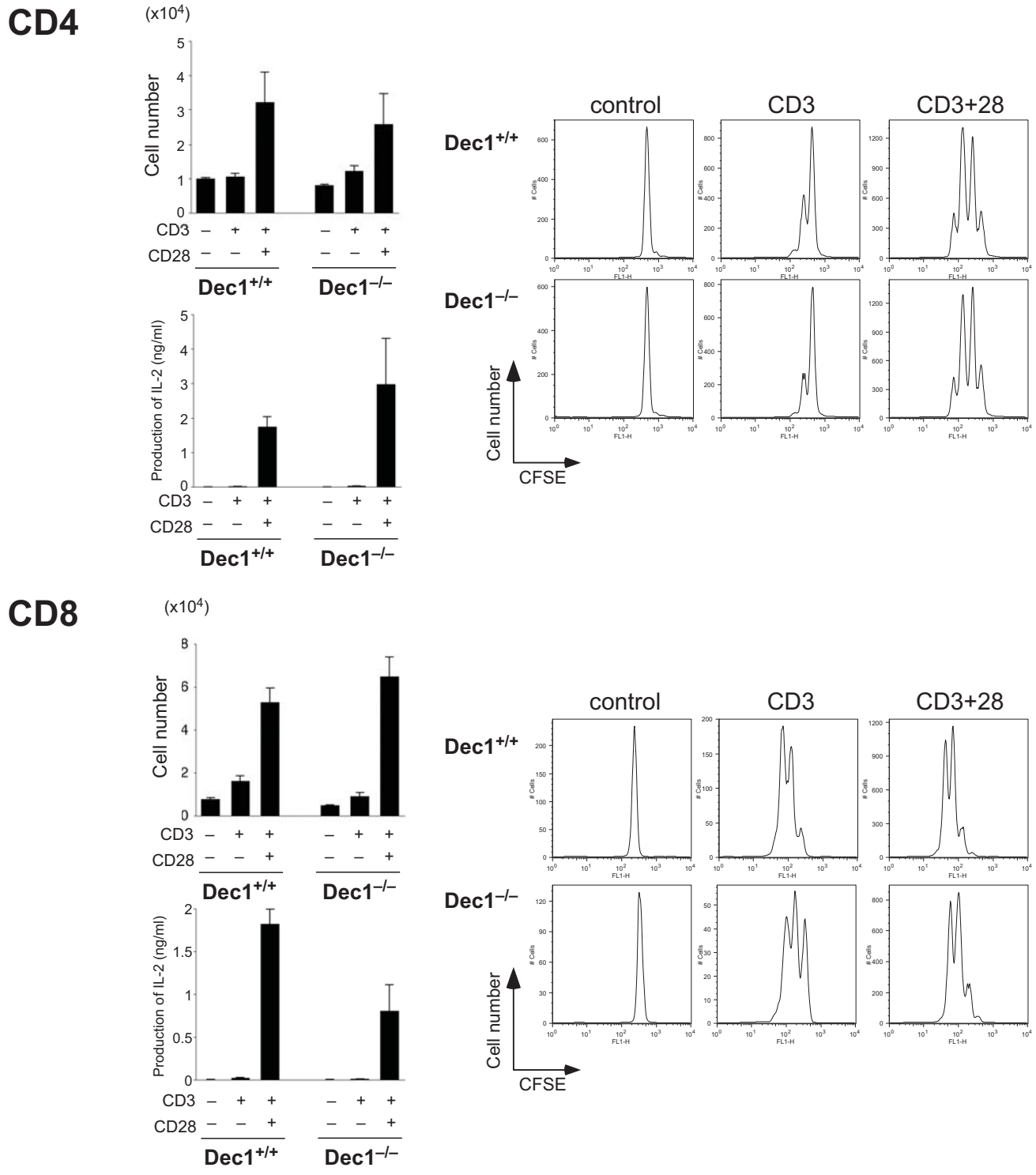

Figure S1

Cell proliferation and IL-2 production of CD4 or CD8 T cell upon TCR stimulation in Dec1$^{-/-}$ mice. Purified CD4^{+}CD25^{-}CD62L^{high} or CD8^{+}CD62L^{high} T cells from were Dec1$^{+/+}$ or Dec1$^{-/-}$ mice were labeled with CFSE, and stimulated with plate-bound anti-CD3 plus anti-CD28Abs (5μg/ml). After 72h, cell were harvested, counted, and analyzed for CFSE dilution by flow cytometry. Concentration of IL-2 in the supernatants was determined by Cytometric Beads Assay (BD). Data represent the mean ±SD from three wells.

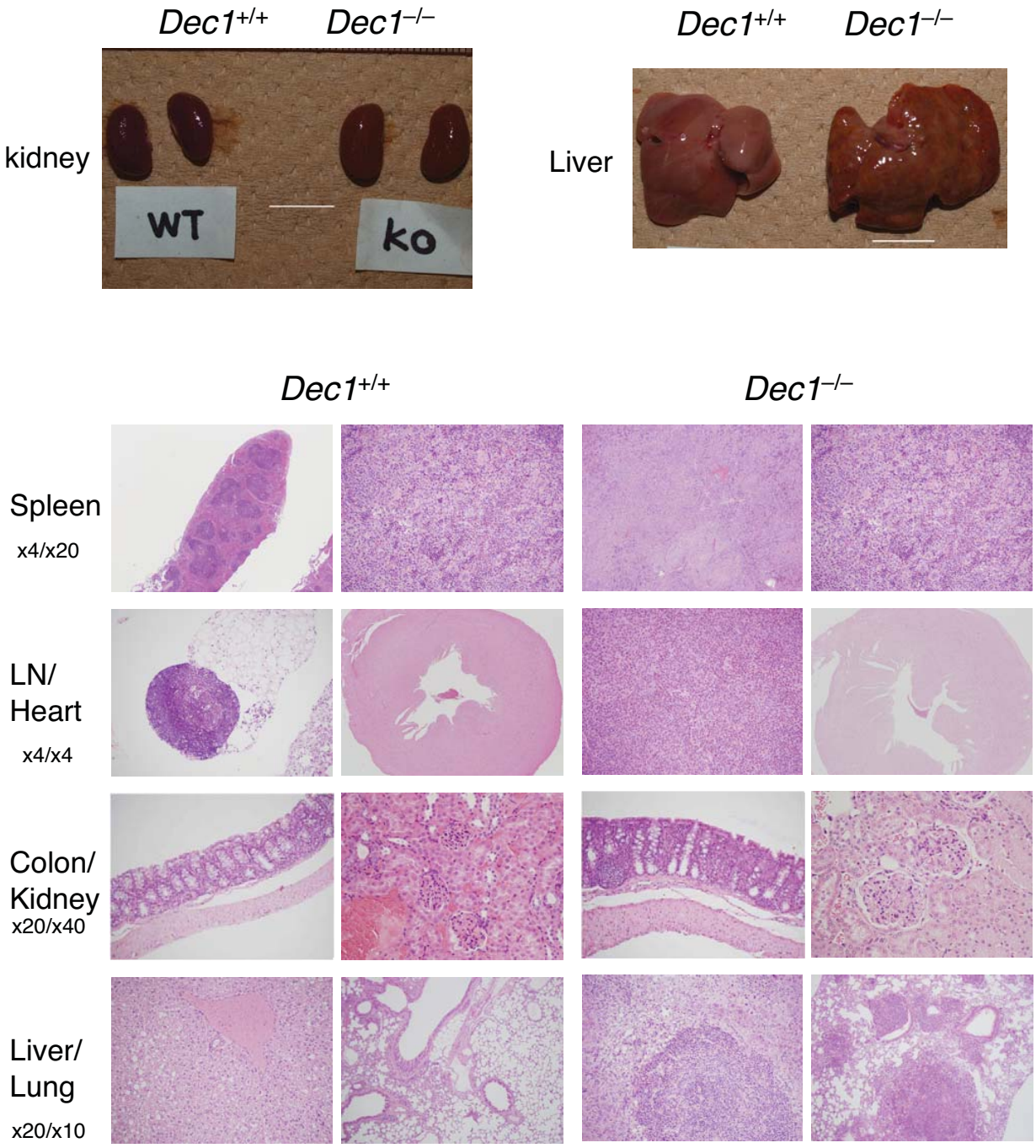

Figure S2
Histological analysis of *Dec1*$^{-/-}$ mice with lymphadenopathy. (upper) Morphology of Kidney and Liver. White bars represent 10mm. (lower) Representative hematoxylin-eosin (H&E)-stained sections of spleen, LN, Heart, Colon, Kidney, Liver and Lung from *Dec1*$^{+/+}$ and *Dec1*$^{-/-}$ mice are shown. Numbers represent the magnification.

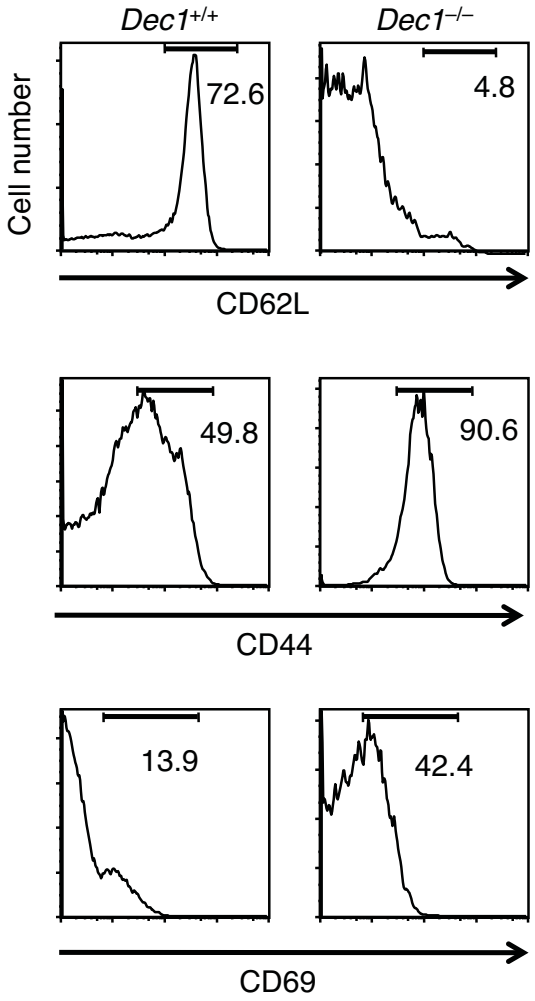

Figure S3
T cell activation in *Dec1*$^{-/-}$ mice with lymphoproliferative disease. Flow cytometric analyses of CD62L, CD44, CD69 expression in CD4 T cells from 1.2-year-old *Dec1*$^{-/-}$ mice with lymophadenopathy or littermate *Dec1*$^{+/+}$ mice are shown. Numbers beneath bracketed lines indicate percentage of positive cells.

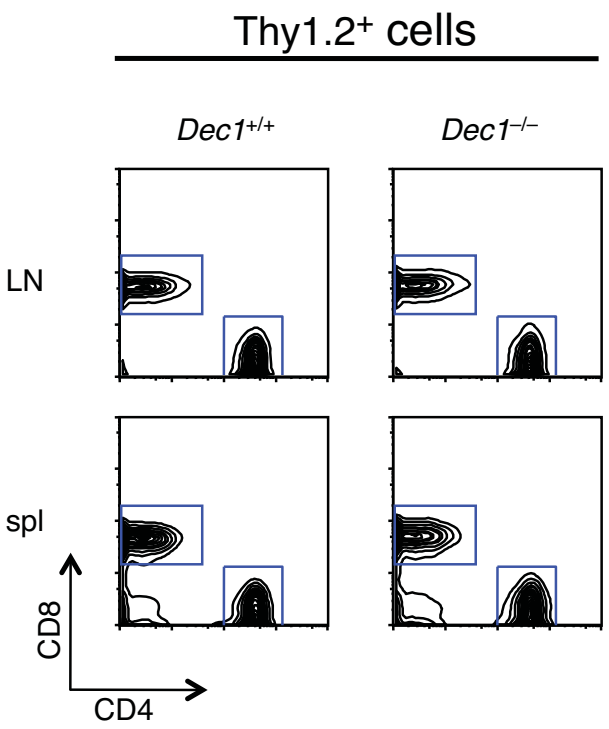

Figure S4
No accumulation of CD4⁻CD8⁻ (DN) T cells in peripheral lymphoid organs in 1.2-year-old *Dec1*$^{-/-}$ mice. Flow cytometric analysis of CD4 versus CD8 expression gated on Thy1.2⁺ T cells in spleen and lymph node are shown.

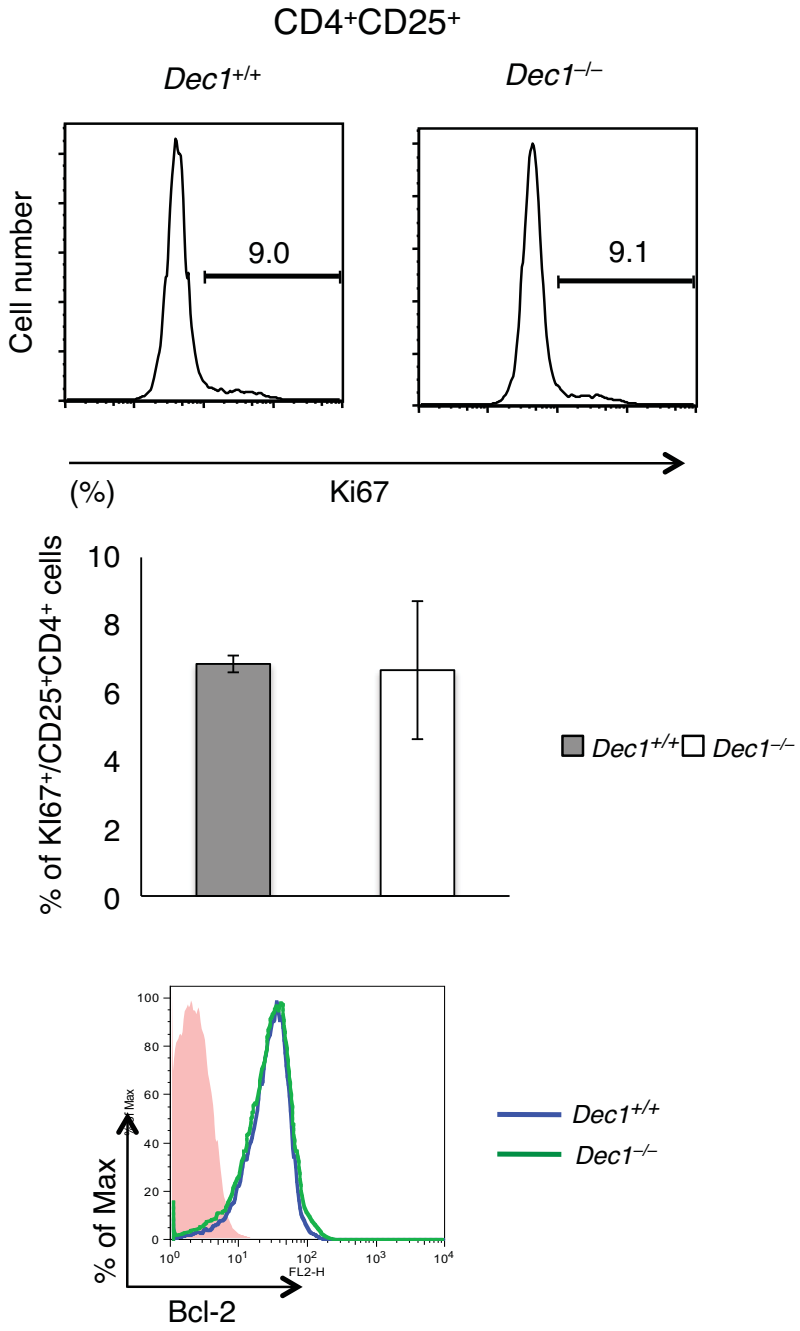

Figure S5

Proliferative status and bcl-2 expression of Treg cells in Ki67 expression in young or aged *Dec1*$^{-/-}$ mice. Ki67 expression of CD4$^+$CD25$^+$ Treg cells from 12-week-old *Dec1*$^{+/+}$ or *Dec1*$^{-/-}$ mice (upper). Numbers above bracketed line indicate percent Ki67 positive cells in CD4$^+$CD25$^+$ cells. The percentage of ki67$^+$ cells among CD25$^+$CD4$^+$ cells in littermate 6-10-month-old *Dec1*$^{+/+}$ or *Dec1*$^{-/-}$ mice (middle). Representative flow cytometric analysis of bcl-2 expression in CD25$^+$CD4$^+$ cells from littermate 6-10-month-old *Dec1*$^{+/+}$ or *Dec1*$^{-/-}$ mice.

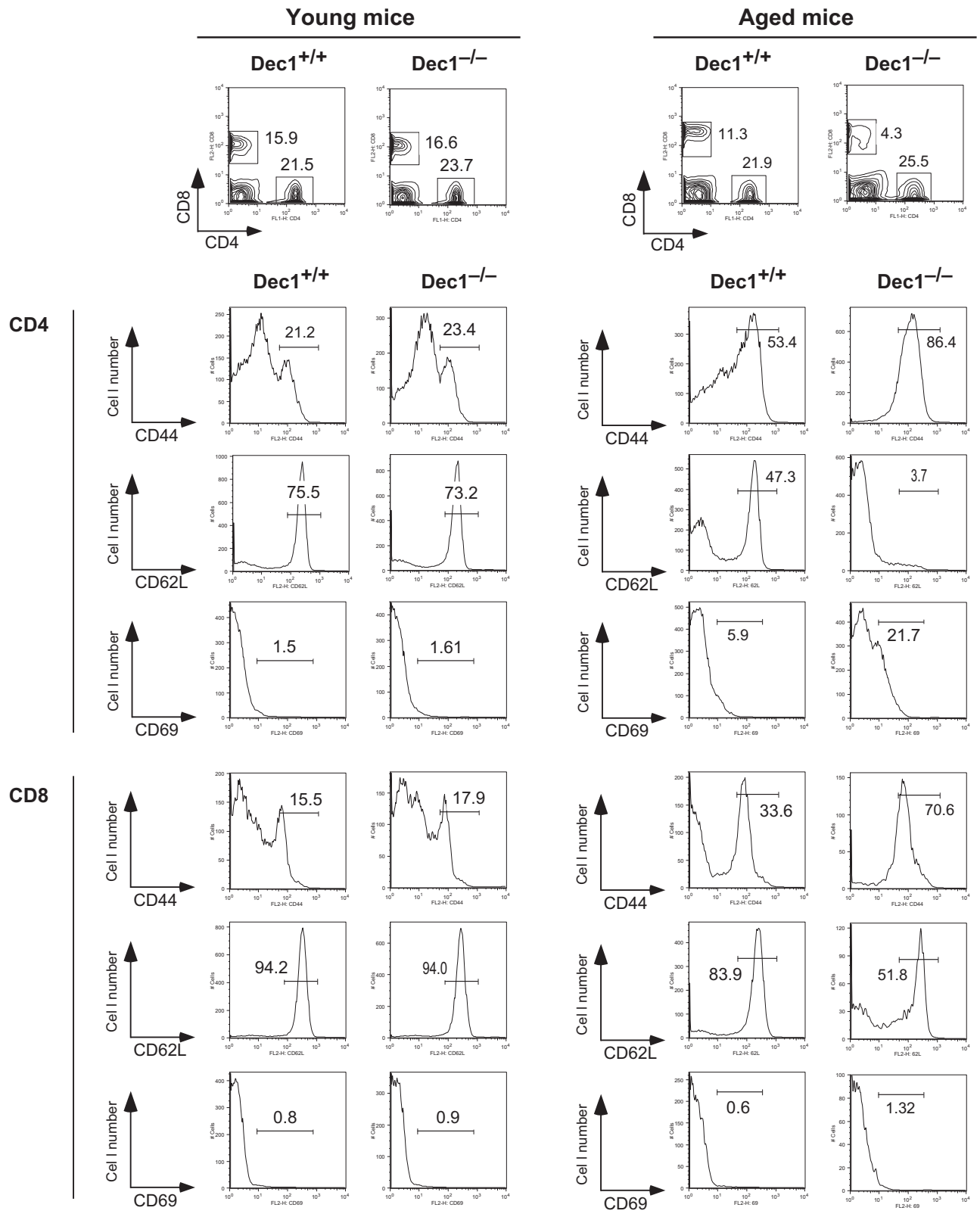

Figure S6

Activated T cells in aged but not young Dec1$^{-/-}$ mice. Representative flow cytometric analyses of CD44, CD62L, and CD69 expression in CD4 and CD8 T cells from 12-week-old (young) and 10-month-old (aged) Dec1$^{+/+}$ or Dec1$^{-/-}$ mice are shown. More than three independent littermates produced with similar results.

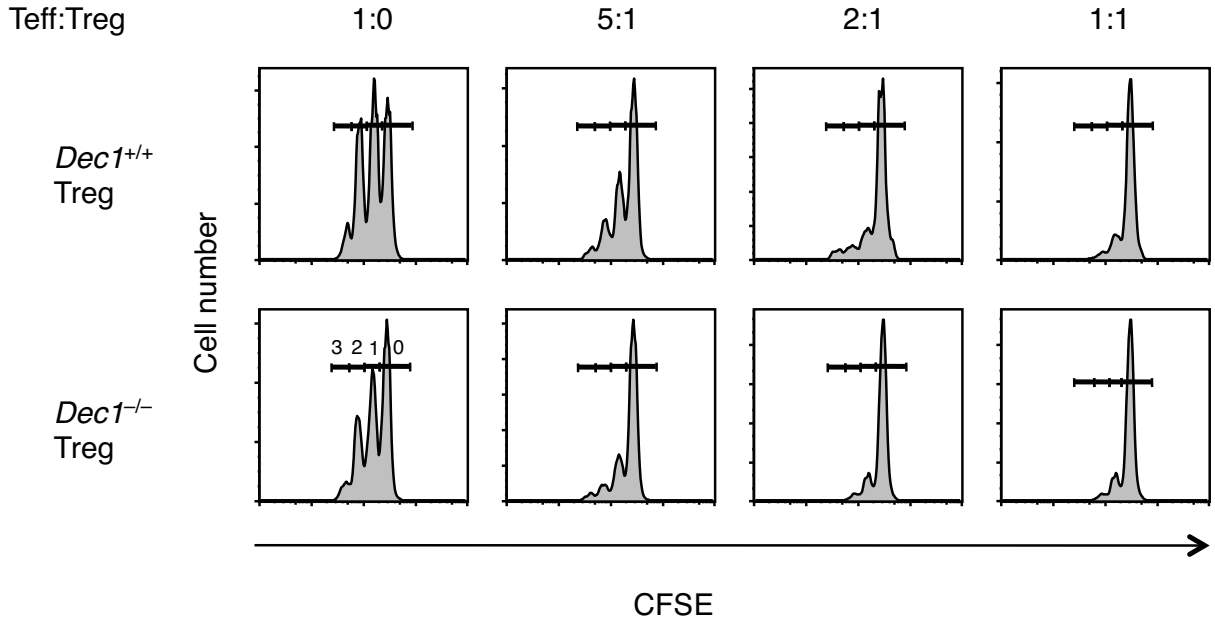

Figure S7
Normal in vitro suppressive function of *Dec1*$^{-/-}$ Treg cells. Representative FACS data in Figure 2A. The percentage of CFSE diluted cells (1-3) was defined as the proportion of dividing cells in Figure 2A

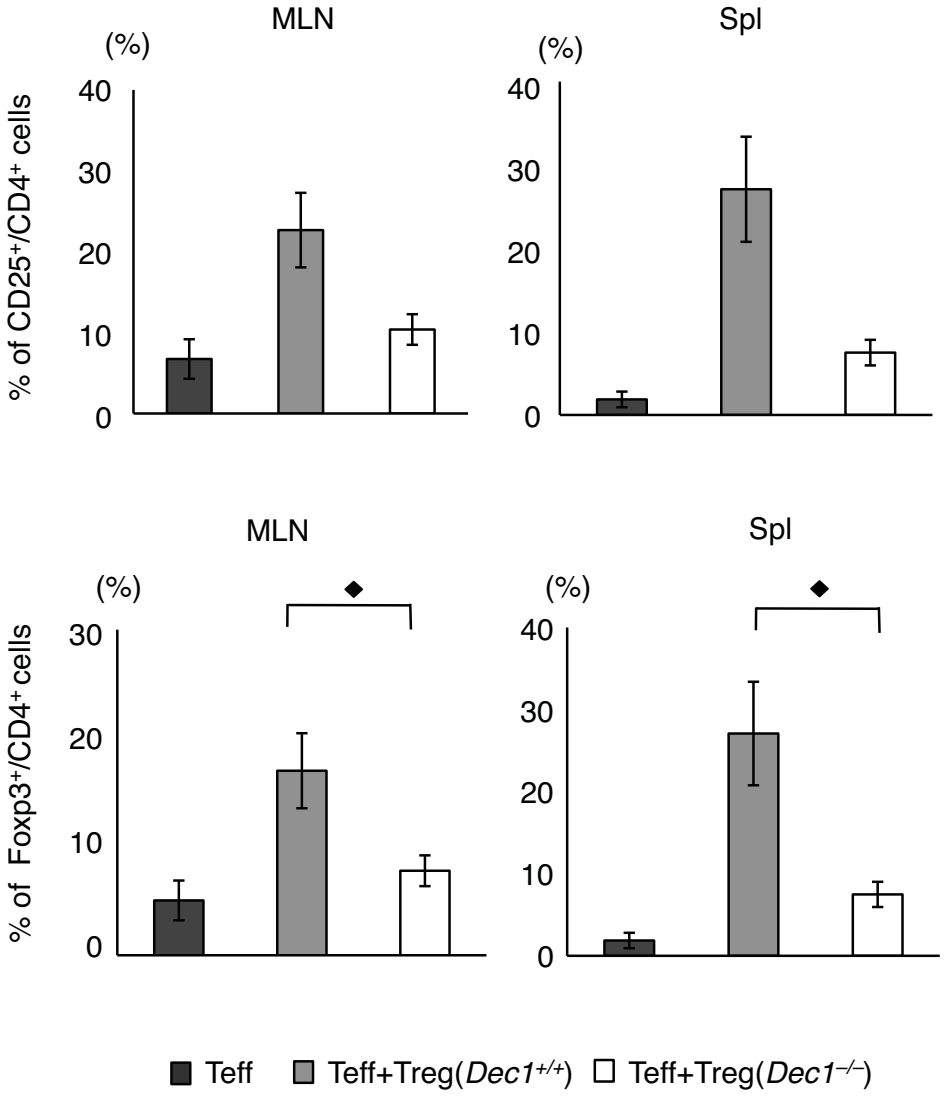

Figure S8
CD4+CD25+ or Foxp3+ cells were reduced in mice transferred with *Dec1*$^{-/-}$ Treg cell. The percentage of CD25^{+} (upper) or Foxp3^{+} (lower) cells among CD4^{+} cells in mesenteric LN (MLN) and spleen (Spl) at 10 weeks after transfer in Figure 2b. ♦, $p<0.01$, t test.

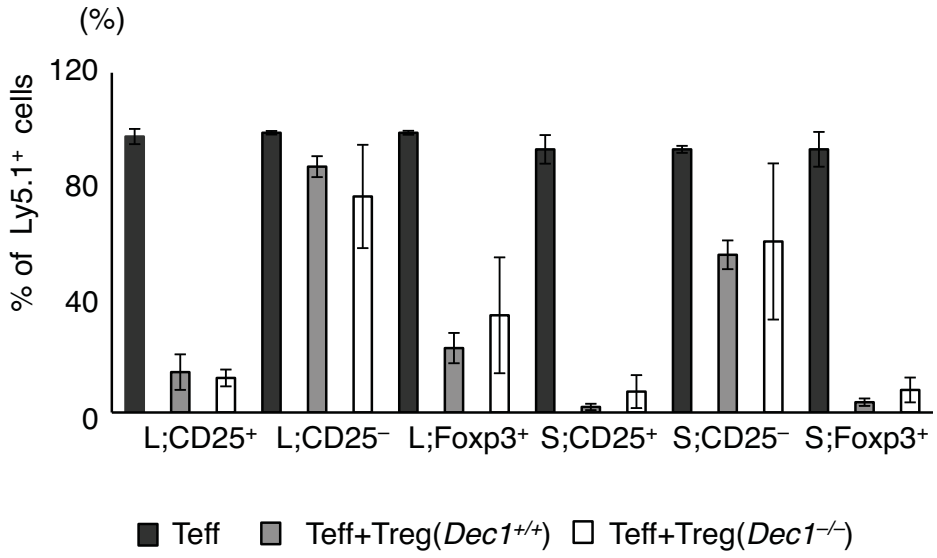

Figure S9
The percentage of Ly5.1$^+$ cells in CD25$^+$, CD25$^-$, or Foxp3$^+$CD4$^+$ cells in Figure 2b.
The graph shows the percentage of Ly5.1 cells in Lymph node (L) or spleen (S) CD4 T cell populations.

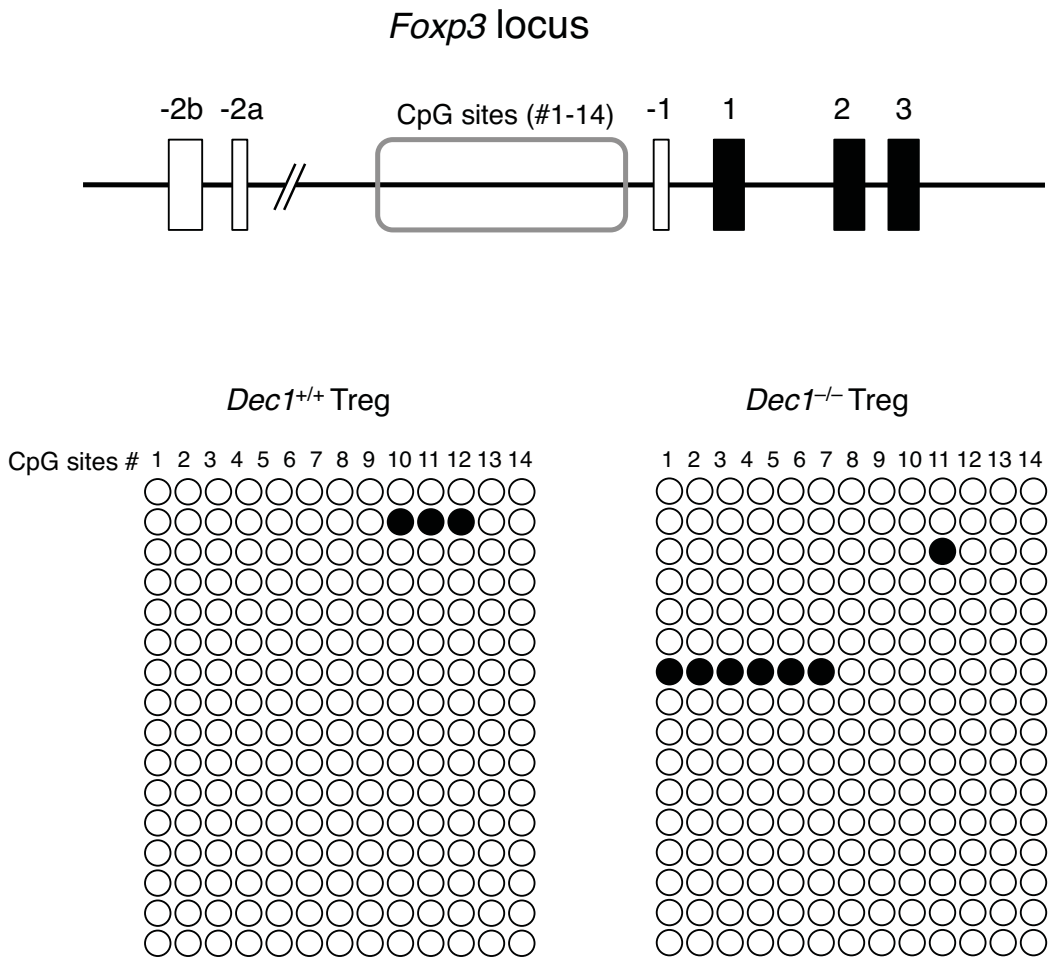

Figure S10
Demethylation status of CpG motifs within the *foxp3* locus in CD4⁺CD25⁺ Treg cells from *Dec1*$^{+/+}$ and *Dec1*$^{-/-}$ mice. (upper) Schematic view of foxp3 locus shows the CpG-rich region upstream from exon1, in which CpG Motifs are highly demethylated in Treg cells but methylated in non-Treg cells. Bisulfate-treated DNA from *Dec1*$^{+/+}$ and *Dec1*$^{-/-}$ Treg cells was sequenced at this region. Methylated CpGs (closed circles) and unmethylated CpGs (open circles) are shown for representative examples of 16 alleles. Each circle represents an individual CpG motif.

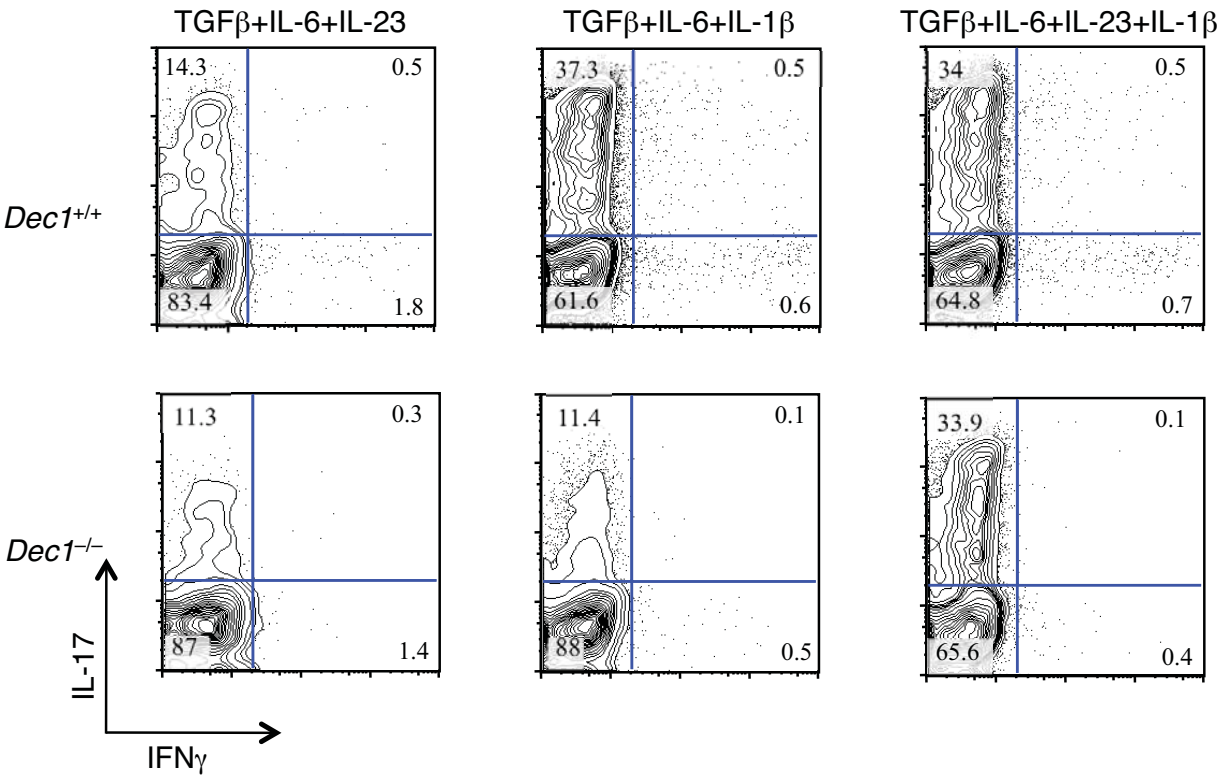

Figure S11

The development of IL-17-producing CD4 T cells derived from *Dec1*$^{-/-}$ naïve CD4 T cell. Purified CD4^{+}CD25^{-}CD62L^{high} T cells were stimulated with anti-CD3ε antibody in the presence of irradiated B6 splenocytes and indicated cytokines for 5 days. After stimulation, cells were restimulated with PMA and ionomycin for 5 h and GolgiStop (last 2h) and were then subjected to intracellular cytokine staining for IL-17 and IFNγ. Numbers in quadrants represent the percentages.

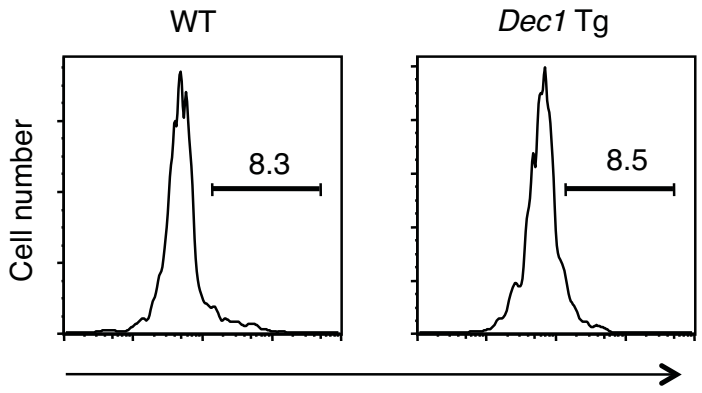

Figure S12
Proliferative status of Treg cells in Ki67 expression in *Dec1* Tg mice. $CD4^+CD25^+$ Treg cells from 12-week-old wild-type or *Dec1* Tg mice. Numbers above bracketed line indicate percent Ki67 positive cells in $CD4^+CD25^+$ cells.

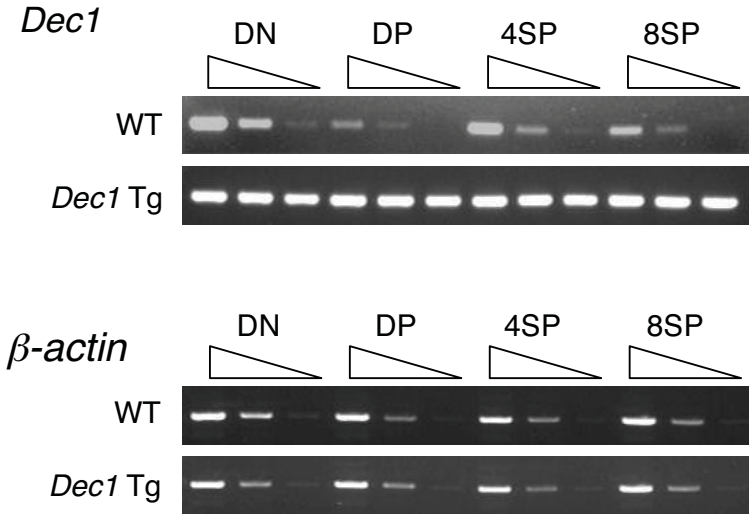

Figure S13
Enhanced expression of *Dec1* mRNA in *Dec1* Tg thymocyte. Semi-quantitative RT-PCR analyses of *Dec1* and *b-actin* mRNA expression in the developmental fractions.

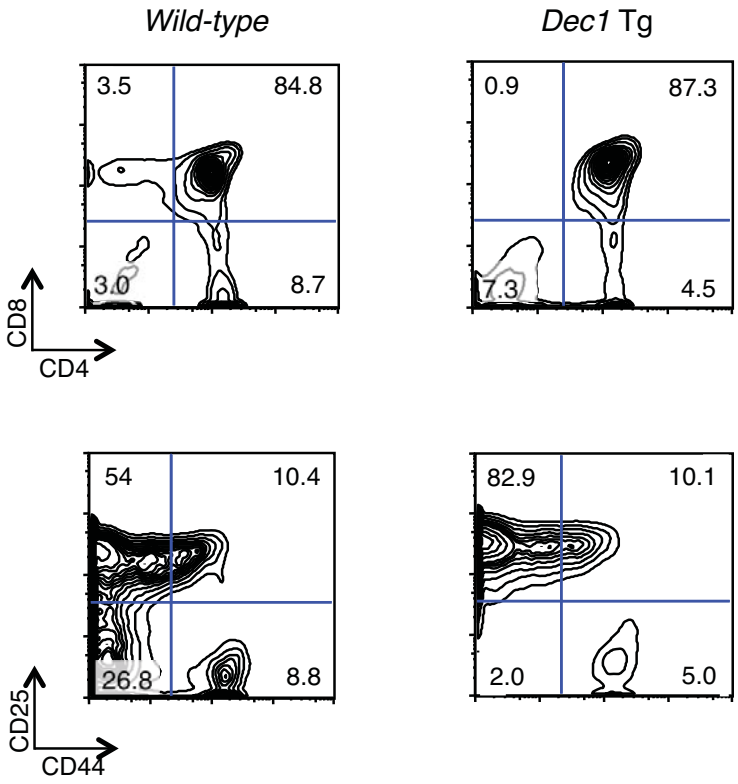

Figure S14

Thymocyte differentiation was affected in Dec1 Tg mouse. Representative flow cytometric analyses of CD4 versus CD8 expression on total thymocytes (upper) and of CD44 versus CD25 expression on lineage (CD4, 8, 3, B220, Mac1, Gr1, Ter119, Nk1.1)-negative thymocytes (lower) from 8-12-week-old *Dec1* Tg and littermate control mice are shown. Numbers in quadrants represent the percentages. The results are representative of two independent *Dec*1 Tg mouse lines.

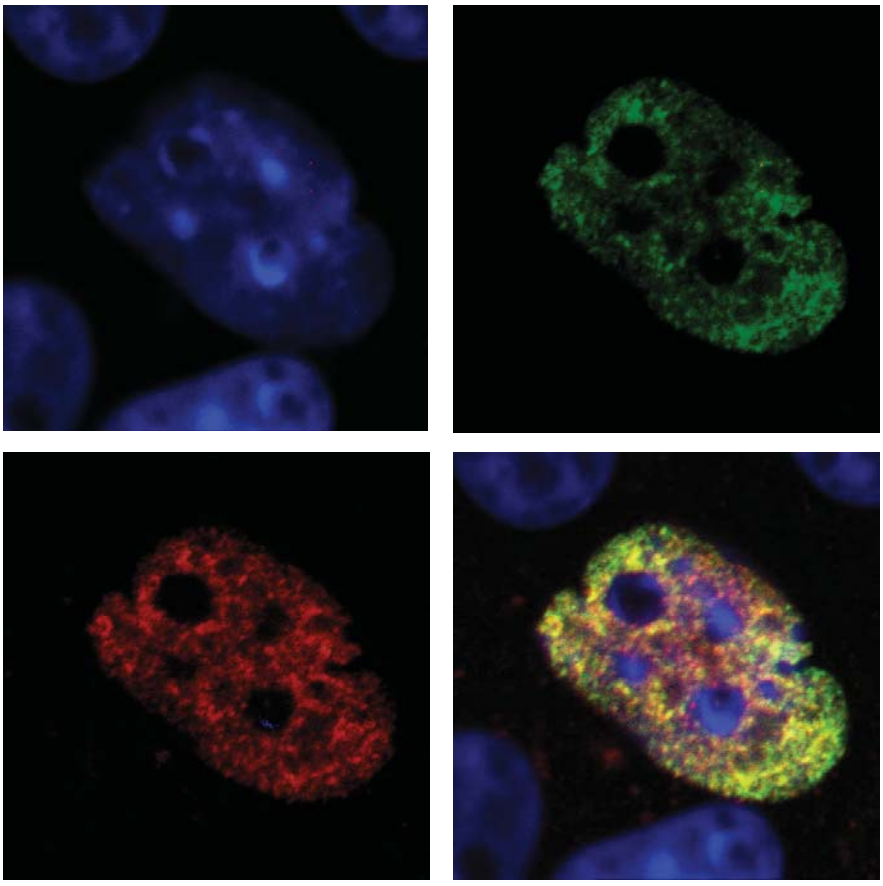

Blue: DAPI Green: Runx1 Red: Dec1

Figure S15

Dec1 and Runx1 were co-localized in nucleus. 293T cells were transfected with vectors encoding Flag-tagged Dec1 or HA-tagged Runx1. 24 h after transfection, cells were fixed with paraformaldehide and permiabilized, and then stained with anti-Flag (Dec1: red) and anti-HA (Runx1: green) antibodies and Hoechist 33342 (DAPI: blue).